Journal of Volcanology and Geothermal Research 291 (2015) 1–13

Contents lists available at ScienceDirect

Journal of Volcanology and Geothermal Research

journal homepage: www.elsevier.com/locate/jvolgeores

Impact of effusive eruptions from the Eguas–Carvão fissure system, São Miguel Island, Azores Archipelago (Portugal)

Dario Pedrazzi [a,b,*], Annalisa Cappello [c], Vittorio Zanon [d,e], Ciro Del Negro [c]

[a] Institute of Earth Sciences Jaume Almera, Group of Volcanology, SIMGEO (UB-CSIC), c/ Lluís Solé i Sabarís s/n, 08028 Barcelona, Spain
[b] Centro de Geociencias, Universidad Nacional Autónoma de México, Campus Juriquilla, Querétaro, Qro. 76230, México
[c] Istituto Nazionale di Geofisica e Vulcanologia, Sezione di Catania, Piazza Roma 2, 95125 Catania, Italy
[d] Centro de Vulcanologia e Avaliação de Riscos Geológicos, Rua Mãe de Deus, 9500-801 Ponta Delgada, Portugal
[e] Institut de Physique du Globe de Paris, 1, rue Jussieu, 75005 Paris, France

ARTICLE INFO

Article history:
Received 17 September 2014
Accepted 10 December 2014
Available online 24 December 2014

Keywords:
Basaltic eruptions
Numerical simulations
Eruptive scenario
Lava flow hazard
Volcanic risk

ABSTRACT

The hazard and risk posed by future effusive eruptions from the Éguas–Carvão fissure system in São Miguel Island (Azores Archipelago) are assessed. This fissure system, located ~13 km from the town of Ponta Delgada and its international airport, was the only site in the whole island to be characterized by recurrent basaltic eruptions over the past 5000 yr. Here we report on the stratigraphic record of these Holocene eruptions, with special mention to both areas and volumes of deposits, and eruptive styles and recurrence. These basic data then are used to constrain numerical simulations of lava flow paths using the MAGFLOW model, after which hazard zones of possible future events are proposed. The lava flow risk is evaluated by combining the hazard with the exposed value, referred to the population, infrastructures and land use. These results are shown in two distinct maps, where the areas most prone to lava flow inundation and the extent of damages in case of a future effusive eruption are identified. We find that lava flows issuing from the Éguas–Carvão fissure system may be a threat to the villages of Feteiras, Capelas and Santo Antonio. Although this study was conducted on the Éguas–Carvão fissure system, the approach used can be applied to the whole São Miguel Island.

© 2015 Elsevier B.V. All rights reserved.

1. Introduction

The Holocene eruptive history of the volcanoes of the Azores Archipelago was up to now analyzed only to evaluate the risk posed by a possible explosive event from the composite volcanoes of Sete Cidades, Água de Pau and Furnas (Moore, 1990; Johnson et al., 1998; Cole et al., 1999, 2008; Guest et al., 1999; Queiroz et al., 2008). However, only three out of 27 eruptions in the Azores were produced from these volcanoes since the Portuguese settling in the 15th century (i.e., Furnas in 1445 and in 1630, and Água de Pau in 1563), and involved the explosive eruptions of silicic magmas. Due to the great danger related to eruptions from a central composite volcano, many studies focused on them (e.g. Moore, 1990; Cole et al., 2008; Queiroz et al., 2008), neglecting the possible consequences due to lava flows. Nevertheless, two effusive eruptions occurred on São Miguel Island in 1563 and in 1652 and damaged the small villages of Ribeira Seca and Rabo de Peixe (Ferreira, 2000).

During the last 10,000 yr one of the most active areas in São Miguel Island was the Éguas–Carvão fissure system, on the southeastern flank of the Sete Cidades Volcano (Fig. 1). The lava flows emitted from closely-spaced fissures were voluminous (more than 10 million of cubic meters) and long enough (over 4 km) to reach the sea at both the northeast and the southwest coasts. This area is located only 13 km northwest from the main town of Ponta Delgada, with a population of ~65,000 inhabitants, and its international airport. The growth in the population and the land exploitation nearby this volcanic system has increased the potential impact of eruptions on the island's economy. The increasing exposure of a larger population and infrastructure is often derived from a poor assessment of the volcanic hazard, allowing inappropriate land use in vulnerable areas. Therefore, a quantitative analysis of the most likely future lava flow paths could be a useful tool to reduce the economic loss from volcanic eruptions through correct land use in densely urbanized areas (Kauahikaua et al., 1995; Felpeto et al., 2001; Crisci et al., 2010).

Here, we present the first quantitative assessment of the impact of lava flows from the Éguas–Carvão fissure system on the community living on São Miguel Island. At first, we have estimated the hazard posed by future effusive eruptions from the Éguas–Carvão fissure system by combining numerical simulations of lava flow paths, spatial probability of vent opening, and event probabilities associated with classes of expected eruptions (Cappello et al., 2011a,b; Del Negro et al., 2013). Then, we have evaluated the risk associated with lava flows from Éguas–Carvão, by classifying areas according to the spatial probability of lava inundation and the expected damage at each point (Gehl et al., 2013). Two maps have resulted from our analysis: the hazard map,

* Corresponding author at: Centro de Geociencias, Universidad Nacional Autónoma de México, Campus Juriquilla, Querétaro, Qro. 76230, México.
E-mail address: dpedrazzi@geociencias.unam.mx (D. Pedrazzi).

http://dx.doi.org/10.1016/j.jvolgeores.2014.12.012
0377-0273/© 2015 Elsevier B.V. All rights reserved.

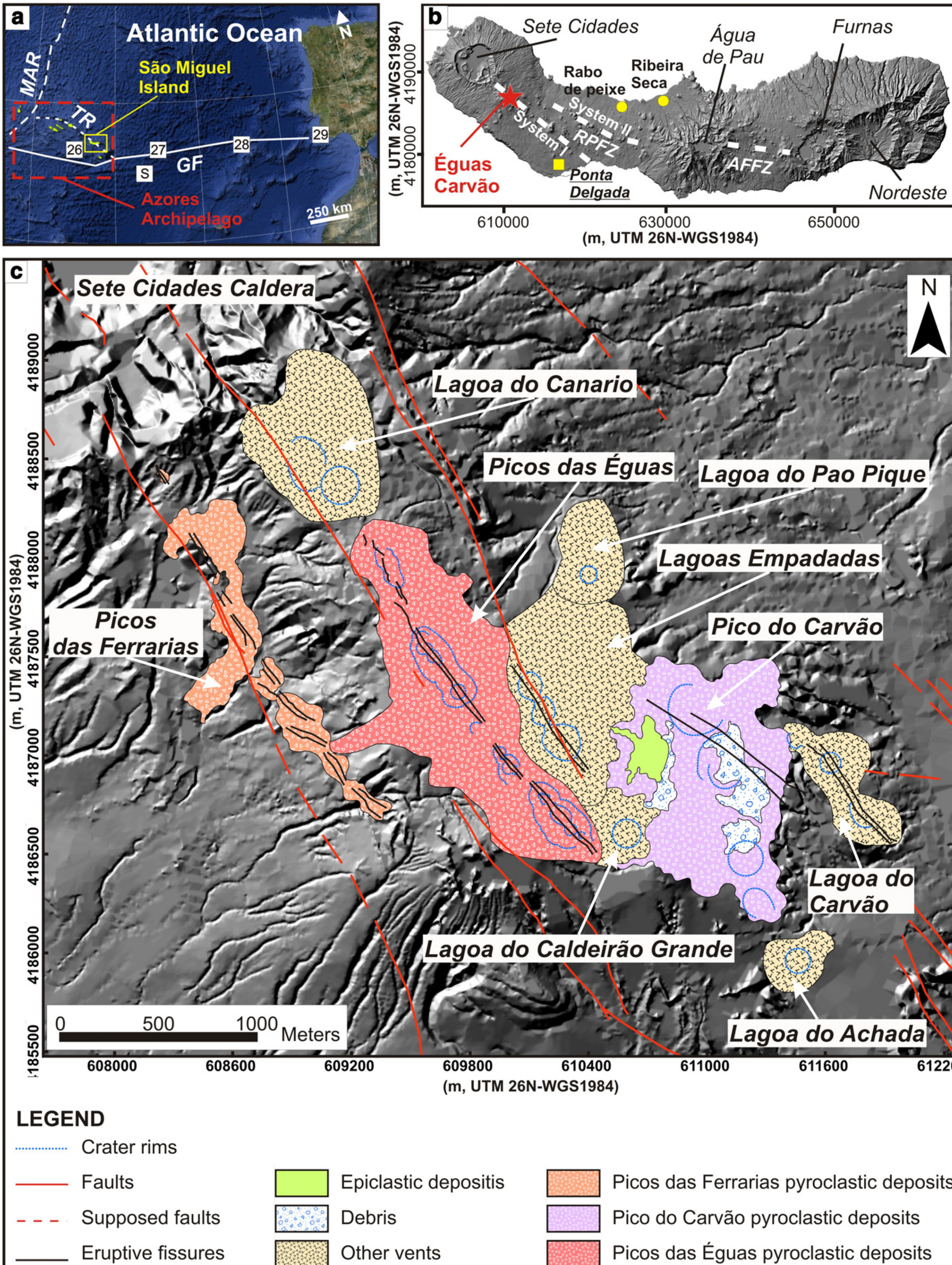
a
Atlantic Ocean
N
MAR
São Miguel
Island
TR
26
27
28
29
S
GF
Azores
Archipelago
250 km
b
Sete Cidades
Água
de Pau
Furnas
Rabo
de peixe
Ribeira
Seca
System II
System I
RPFZ
AFFZ
Éguas
Carvão
Ponta
Delgada
Nordeste
(m, UTM 26N-WGS1984)
4190000
4180000
610000
630000
650000
(m, UTM 26N-WGS1984)
c
Sete Cidades Caldera
N
Lagoa do Canario
Picos das Éguas
Lagoa do Pao Pique
Lagoas Empadadas
Pico do Carvão
Picos
das Ferrarias
Lagoa do
Carvão
Lagoa do Caldeirão Grande
Lagoa do Achada
0
500
1000
Meters
4189000
4188500
4188000
4187500
4187000
4186500
4186000
4185500
(m, UTM 26N-WGS1984)
608000
608600
609200
609800
610400
611000
611600
612200
(m, UTM 26N-WGS1984)
LEGEND
Crater rims
Faults
Supposed faults
Eruptive fissures
Epiclastic depositis
Debris
Other vents
Picos das Ferrarias pyroclastic deposits
Pico do Carvão pyroclastic deposits
Picos das Éguas pyroclastic deposits

showing the probability that a certain area will be inundated by future lava flows, and the risk map, highlighting the likely damage associated with a possible effusive event.

2. Geological setting and volcanism at São Miguel Island

The Azores islands are the emerged peaks of a series of composite volcanic edifices located in the central-north Atlantic Ocean, at the boundary between Eurasian, Nubian and American tectonic plates. This area accommodates the stresses generated by the differential movements of these plates through a series of tectonic structures of regional importance (e.g., Marques et al., 2013). The Terceira Rift is the longest of these structures, which extends with a general WNW–ESE direction, for about 500 km and is intersected by sets of transtensional faults (e.g., Madeira and Ribeiro, 1990; Madeira and Brum da Silveira, 2003). The differential movements of these latter faults generated en-echelon basins and horst and graben structures (Lourenço et al., 1998; Miranda et al., 1998). The intersection of the Terceira Rift with faults striking 150°E favored the formation of shallow magma reservoirs that fed the activity of composite stratovolcanoes (Luis et al., 1998).

The island of São Miguel is located almost at the eastern end of the Terceira Rift (Fig. 1a) and is formed by three young caldera-dominated quiescent stratovolcanoes and the remnant of the volcano of Nordeste, at the eastern end of the island (Fig. 1b). The magmatism of these volcanoes during the last 10,000 yr was typically explosive, with the emission of highly evolved magma from the summit calderas, and also by small-volume eruptions of relatively primitive magmas along radial fractures (e.g., Beier et al., 2006).

Stratovolcanoes are separated by areas of extensional tectonics (Fig. 1b), which accommodate the deformation at local scale through a series of normal faults and fissural volcanism (Lourenço et al., 1998; Madeira and Brum da Silveira, 2003). Erupted magmas are basaltic to hawaiitic in composition and ascended directly from the Moho Transition Zone at about 29 km (Zanon, in press).

The westernmost of these areas is the Região dos Picos fissure zone (hereinafter named RPFZ), which extends with a WNW–ESE direction for ~22.5 km, between Sete Cidades and Água de Pau volcanoes. Its activity dates back to at least 30,000 B.P. (Moore and Rubin, 1991; Johnson et al., 1998), with eruptions occurring from two fissure systems (named “System I” and “System II” by Zanon, in press—Fig. 1b). System I departs from the upper ESE flank of Sete Cidades Volcano and runs towards the SE for about 15 km. System II departs from the lower western flank of Água de Pau Volcano and runs for about 18 km towards Sete Cidades with a WNW–ESE direction. These two systems overlap in the central sector of Região dos Picos.

Eastwards, another area of extensional tectonics is the Achada das Furnas fissure zone (hereinafter named AFFZ), which extends for ~7.5 km between the volcanoes of Água de Pau to the west, and Furnas to the east, following a general WNW–ESE direction (Fig. 1b). Magmatism here occurred from 30,000 to 5000 yr B.P. from subparallel fissures (Moore and Rubin, 1991; Johnson et al., 1998), which are now partially buried by thick pumice fallout deposits from stratovolcanoes.

Despite the last eruption at the RPFZ occurred in the central segment of System II, in 1652, most eruptions occurred along the System I during the last 5000 yr. In particular, we have observed recurrent effusive eruptions in the Éguas–Carvão area, in the northwestern tip, about 2 km SE of the Sete Cidades caldera (Fig. 1b). Here we have recognized an irregular elevation profile due to the presence of a large volume of accumulated lava (Fig. 2b, c), compared to other sectors of the island (Fig. 2d, e). The Éguas–Carvão fissure system developed outside of the graben structure, in a NW–SE direction, and intersected the caldera of Sete Cidades (Fig. 1c). Mafic magmas from the Éguas fissure, the Lagoa Empadadas maar, the Lagoa do Caldeirão Grande tephra ring, and from the Pico do Carvão fissure (Fig. 1c), partially filled the graben and created the local topographic high (Fig. 2b, c). The Picos das Ferrarias fissure (Fig. 1c) is located slightly off-axis but it is still part of this system due to similar spatial characteristics of the fissure and the petrography of the products. The cones related to these eruptions are very close to each other, and in some cases coalesced or partially overlapped, to generate complex pyroclastic sequences. The dispersal of the pyroclastic products from these eruptions is limited to a few hundred meters around the fissure system (Fig. 1c), while lavas flowed for several kilometers, reaching both the northeast and southwest coasts of the island (Fig. 3).

3. Eruptions from the Éguas–Carvão fissure system

We reconstructed the volcanic history of the Éguas–Carvão fissure system by integrating field surveys with the interpretation of the recent digital orthophotos at 1:5000 scale. Moreover, we discriminated the characteristics of emitted lava through petrographic observations.

The description of the units has followed lithostratigraphic criteria from the oldest to the youngest and allowed identifying and mapping three main lava flows erupted from the Éguas–Carvão fissure system in the last 3000 yr. A distribution map of pyroclastic deposits (Figs. 1c and 3) and lava flows (Fig. 3) for each emission center has been drawn at a scale of 1:5000 for an area of ~20 km^2. Systematic sampling of erupted products has been also carried out for a discrimination of the flow units, especially where lush vegetation and recent pyroclastic fallout deposits from the nearby Sete Cidades Volcano were present. The relative ages of deposits from each volcanic center have been determined on the basis of published age of fallout deposits from Sete Cidades Volcano and lava flow units (Moore and Rubin, 1991; Queiroz et al., 2008).

3.1. Picos das Éguas Unit (2700 ± 250 yr B.P.)

This unit consists of reddish welded spatter, ranging in size from lapilli to bombs, and stratified lapilli beds with Pele's hairs. Armored bombs (Ø < 18 cm), consisting of ultramafic and syenitic nodules, described by Mattioli et al. (1997), are common. The base of the sequence is not visible, while at the top there is the tephra layer *P11* (*2220 ± 70 yr B.P.*) from Sete Cidades Volcano (Fig. 4).

Two narrow ′a′ā lava flows extend towards both the northeast and southwestern coasts, close to Feteiras and Santo Antonio villages respectively (Fig. 3a). The presence of *P11* stratigraphic marker, the high content of olivine crystals, and the widespread presence of mafic to ultramafic xenoliths are typical features of these flows. The main field characteristics are shown in Table 1.

3.2. Pico do Carvão Unit (1280 ± 150 yr B.P.)

This unit is constituted by well stratified-to massive black lapilli beds of metric to centimetric thickness (Fig. 4), formed by vesicular lapilli and scarce loose crystals. Frequent cm-thick yellowish buchites, produced from the partial melting of pumices existing in the pre-eruptive basement, are also present. The base of the unit is marked by the *P14* (*1860 ± 120 yr B.P.*) and *P15* deposits and the top by the *P17*

Fig. 1. a) Geographical setting of the Azores Archipelago (inside the red dotted square) and São Miguel Island (inside the yellow square); b) digital elevation model of São Miguel Island with the main volcanic systems. Éguas–Carvão fissure system, south of Sete Cidades Volcano, is marked by the red star. RPFZ and AFFZ stand for Picos Region Fissure Zone and AFFZ for Achada das Furnas Fissure Zone, respectively; c) geological map of the Éguas–Carvão fissure system, with the main volcano-tectonic structures.

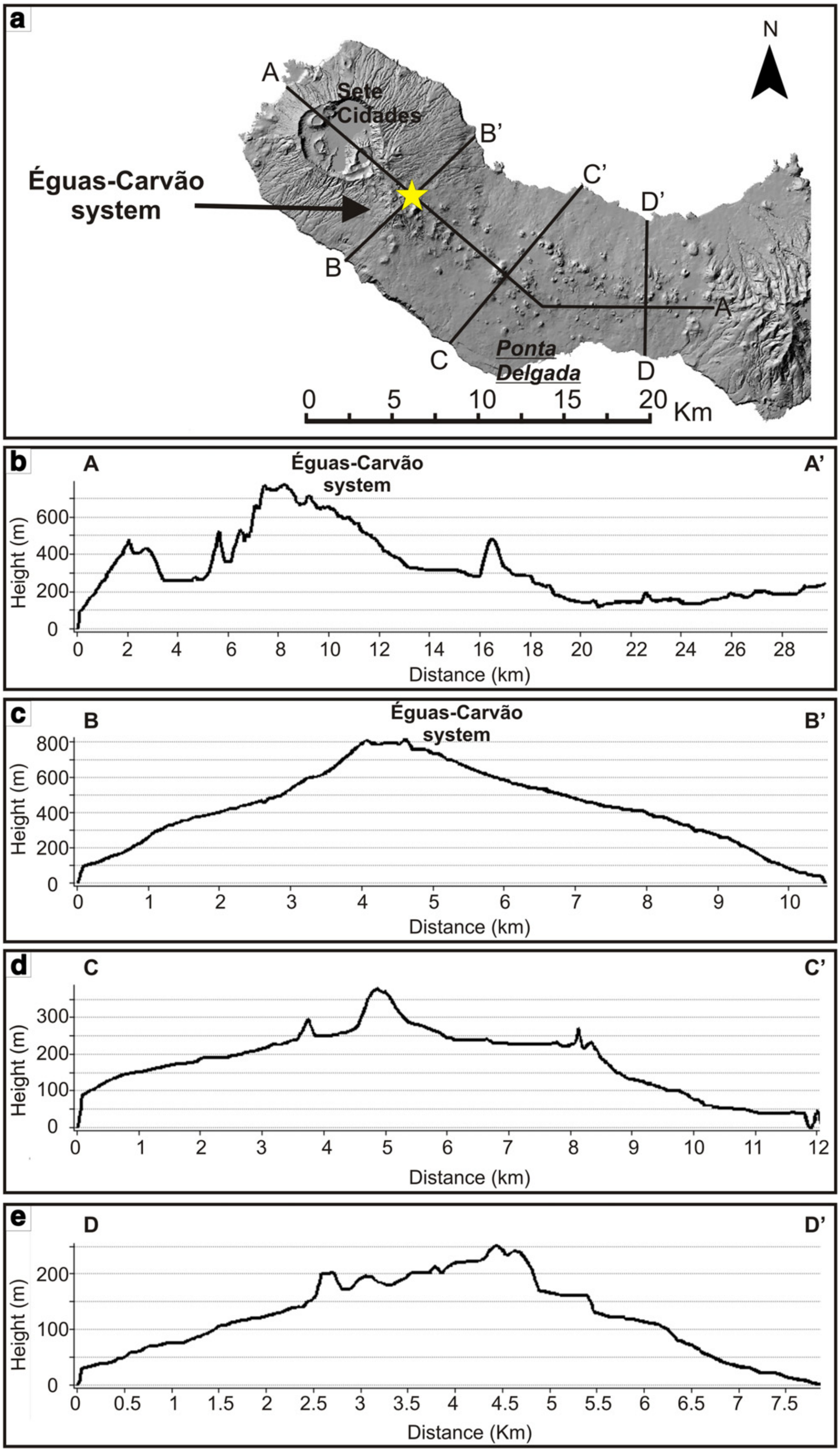

Fig. 2. a) Elevation profiles measured in São Miguel Island: b) A-A′, from Sete Cidades Volcano through Picos Region Fissure Zone; c) B-B′, from south-west to north-east through Éguas–Carvão fissure system; d) C-C′, from south-west to north-east through Central Picos Region Fissure Zone; e) D-D′, from south to north at the eastern Picos Region Fissure. The yellow star marks the location of the Éguas–Carvão fissure system.

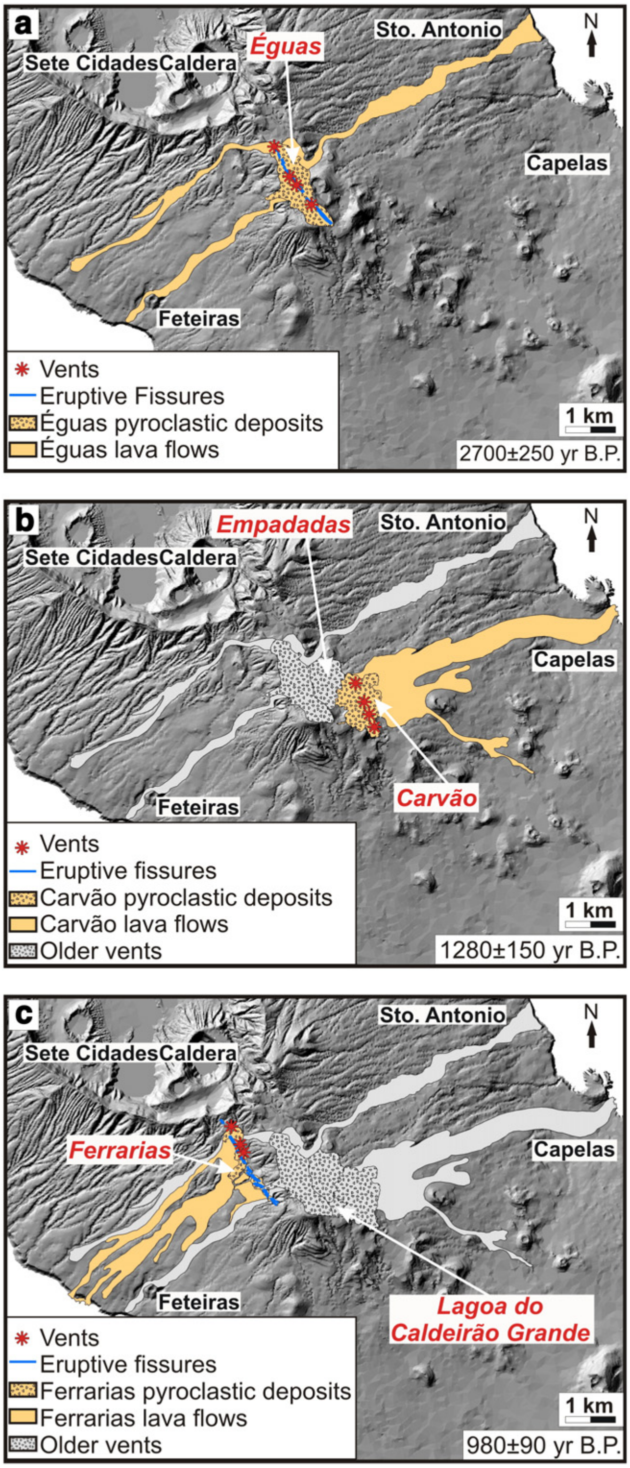

Fig. 3. Simplified maps of volcanic products erupted by Éguas fissure system (a), Carvão fissure system (b), and Ferrarias fissure system (c), retrieved by fieldworks and petrographic analysis of the products sampled from field logs. The blue lines show the location of the fissures related to each volcanic system. Asterisks indicate the location of main eruptive vents.

stratigraphic marker (*500 ± 100 yr B.P.*) and Lagoa do Caldeirão Grande Unit (Fig. 4).

Three flows from this eruption traveled towards NE and SE and only one reached the sea in the NE direction after traveling 5 km (Fig. 3b and Table 1). The ocean entry is a small lava delta located just east of the Capelas tuff cone (Fig. 3b). Lava channels and tumuli suggest a long lasting eruption, with steady-state eruptive conditions (Kilburn, 2000).

3.3. Picos das Ferrarias Unit (980 ± 90 yr B.P.)

A discontinuous welded spatter deposit formed during short-lived fire fountains from NW–SE oriented en echelon fissures, on the southwestern slope of Éguas cone, where hornitos and spatter ramparts are located (Figs. 1c and 3c). This deposit is covered by the *P17* tephra layer (*500 ± 100 yr B.P.*) (Fig. 4), which is the last eruptive episode from Sete Cidades Volcano.

A small 'a'ā lava flow field developed towards the SW coast with numerous small lobes fed by narrow channels. This flow (Table 1) reached the sea in the area of Feteiras village, forming a small lava delta (Fig. 3c). The low lava volume emitted and the simple structure of lava field (e.g., absence of lava tubes, small size of cinder cones) suggest a very short duration of the eruption (Kilburn, 2000).

3.4. Petrographic characterization of lava flows

Lavas from Picos das Éguas Unit are porphyritic with total crystal content (phenocrysts and microphenocrysts) of ~61%, given by clinopyroxene, plagioclase and olivine in order of abundance, and intersertal texture (Fig. 5a). Numerous large (>1 mm) euhedral to subhedral olivines and clinopyroxenes showing disequilibrium features (reaction rims and embayments) are frequent, as are also glomeroporphyritic aggregates of mafic phases. These lavas characteristically contain ultramafic xenoliths of cumulitic origin (clinopyroxenites and dunites) and microcrystalline syenites and few gabbros, which are up to 10 cm across and can be found as armored by a film of volcanic glass.

Lavas from Pico do Carvão Unit are poorly porphyritic (total crystal content ~14%) with intergranular texture (Fig. 5b). Euhedral or skeletal phenocrysts of olivine and rare clinopyroxene and microphenocrysts of mafic phases, plagioclases and oxides constitute the mineral assemblage.

Picos das Ferrarias Unit lavas show a total crystal content of ~36%, given by olivine, plagioclase, clinopyroxene, and oxides. Megacrysts (up to 1 cm) of plagioclase, olivine, and clinopyroxene are also present. The texture is intergranular (Fig. 5c). Numerous small (up to 4 cm) cumulitic dunites and clinopyroxenites are also common, while syenites are absent.

4. Assessment of lava flow hazard

The methodology we have adopted to obtain a reliable and comprehensive assessment of lava flow hazards at São Miguel Island relies upon the MAGFLOW numerical model for simulating lava flow paths (Vicari et al., 2007, 2011; Del Negro et al., 2008; Ganci et al., 2012). Lava flow simulations are based on the knowledge of volcanological eruptive conditions, derived from the integration of historical and geological data (Kereszturi et al., 2014). In particular, this methodology develops through four steps: (i) assessment of the spatial probability of future vent opening, (ii) estimation of the occurrence probability, associated with classes of expected eruptions, (iii) simulation of a large number of eruptive scenarios with the MAGFLOW model, and (iv) computation of the probability that a lava flow will inundate a certain area.

4.1. Spatial probability of vent opening

The computation of the probability of future vent opening is based on the analysis of the spatial distribution of the eruptive fissures in an area around the Éguas–Carvão fissure system, defined on the basis of the presence of fractures (Fig. 1). We have defined a 100-m grid of potential vents v_i on a rectangular area of ~3.8 × 2.5 km and have

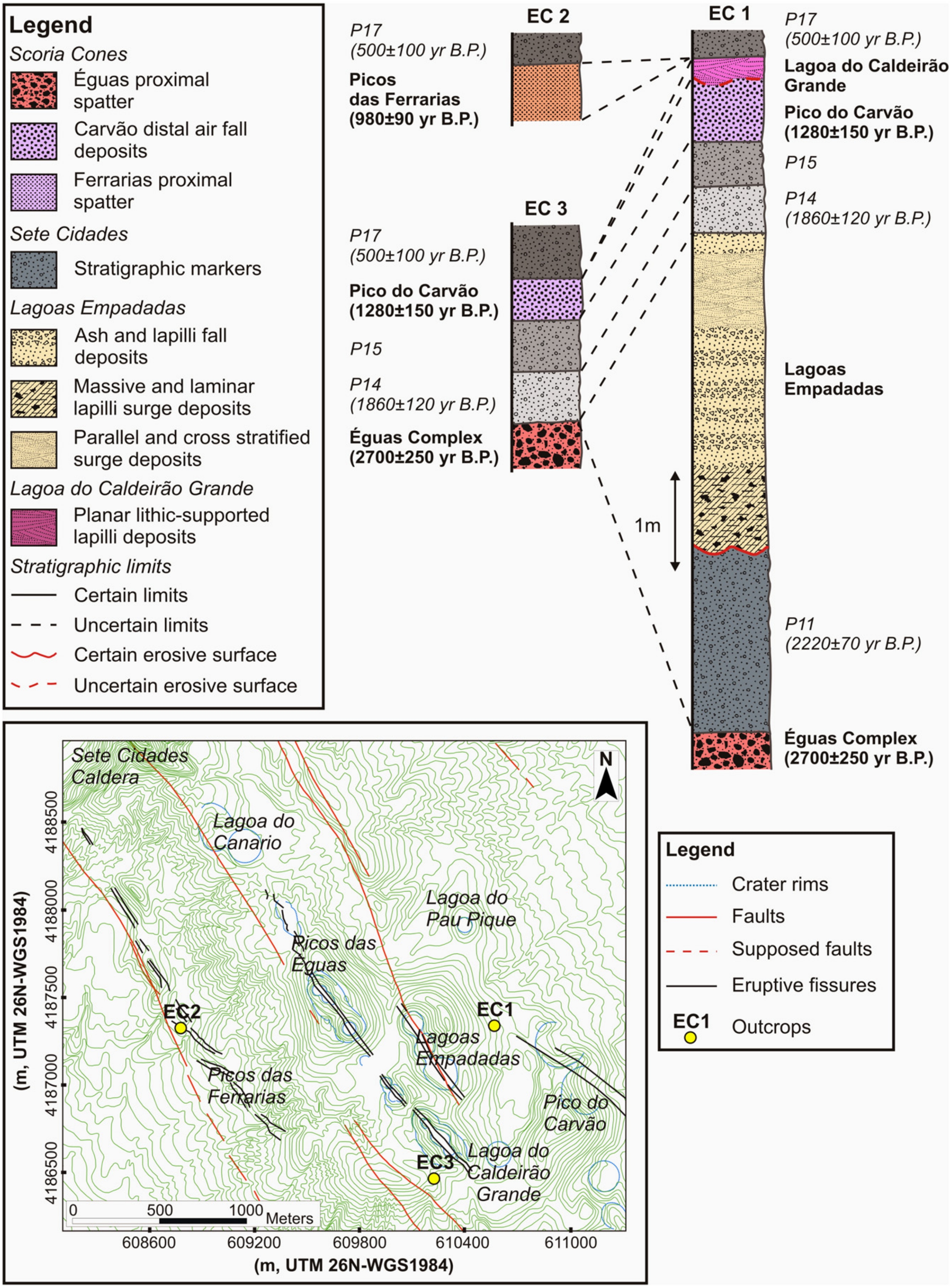

Fig. 4. Sketch of the stratigraphy of the studied volcanic units. The position of the various "P" pumice layers from the Sete Cidades Volcano are marked with different shades of gray. The known ages of the units in the stratigraphic column are placed as well.

Table 1
Main data related to Picos das Éguas Pico do Carvão and Picos das Ferrarias lava flows.

Cones	Altitude (m a.s.l.)	UTM WGS84 Coordinates (m)	Maximum length (km)	Total covered area (km^2)	Range of lava thickness (m)
Picos das Éguas	874	609581E–4187428 N	5	4.4	3–20
Pico do Carvão	786	610987E–4186789N	4.5	4.9	5–15
Picos das Ferrarias	632	608520E–4188102N	5	3.5	3–20

calculated for each v_i a probability density function λ using the Gaussian kernel (Cappello et al., 2012, 2013; Becerril et al., 2013):

$$\lambda_{xy}(v_i) = \frac{1}{2\pi N h^2}\sum_{j=1}^{N} e^{-\frac{d_j^2}{2h^2}} \quad (1)$$

where N is the number of eruptive fissures, d_j is the minimum distance between the potential vent v_i and each segment constituting the j-th eruptive fissure, and h is the smoothing factor or bandwidth. This latter parameter strongly influences the size of λ, giving eruptive fissures high emphasis (for small values of h) or yielding a more uniform distribution across the area (for large values of h). The best estimate for h was found to be 500 m using the Least Squares Cross-Validation (Worton, 1995; Bartolini et al., 2013), which is based on minimizing the integrated square error between the true and the estimated distribution. The function λ is then rescaled so that the integral across the area equals unity. We estimate the events expected per unit area and produce a spatial probability map of new vent opening (Fig. 6a). The resulting distribution of probabilities is non-homogeneous. The highest probability of new eruptions occurs in the area between Picos das Ferrarias and Picos das Éguas.

4.2. Event probabilities associated with classes of expected eruptions

We have derived the classification of expected eruptions from the three main past eruptions occurred at the Éguas–Carvão fissure system (i.e., Éguas, Carvão and Ferrarias). For each lava flow field, we have collected the main quantitative volcanological data, concerning the maximum length, the total covered area, and the range of lava thickness (Table 1).

Furthermore, we have used MAGFLOW model to reproduce the lava flow path of past eruptions, by fitting the lava surface and thickness as a function of emission rate and duration values. In this way, we have distinguished two possible eruptive classes characterized either by short duration, high emission rate (ECL1, Éguas and Ferrarias-like) or long duration, low emission rate (ECL2, Carvão-like). Specifically, we estimated the average values of duration and lava emission rate for both classes: 7 days and 33 m^3/s for ECL1, and 60 days and 9 m^3/s for ECL2. Since the catalog of past eruptions cannot support usual methods of statistical analysis, we assigned to classes ECL1 and ECL2 the same probability of occurrence (0.5) in the estimation of lava flow hazard.

4.3. Lava flow simulations by MAGFLOW model

The MAGFLOW model is based on the Cellular Automata approach, where the evolution function is directly derived from a steady-state solution of the Navier–Stokes equation for Bingham fluids, coupled with a simplified heat transfer model (Herault et al., 2009; Vicari et al., 2009; Bilotta et al., 2012). The main input parameters of MAGFLOW are the digital topography, the physical properties of the lava (e.g., density of lava, emissivity, solidification and extrusion temperatures), the effusion rate, and the location of eruptive vents. As digital representation of the local topography, we have used a 30-m ASTER Global Digital Elevation Model (DEM) Version 2 (ASTER GDEM V2) developed and released by the Ministry of Economy, Trade, and Industry (METI) of Japan and the United States National Aeronautics and Space Administration (NASA).

The physical parameters (Table 2) have been inferred from petrological and chemical properties of the lavas erupted from the Éguas–Carvão fissure system. Densities of lava samples have been measured through a MD 200 s electronic densimeter (error ± 1 kg m^{-3}) and corrected for porosity. Eruptive temperatures have been inferred from literature (Mattioli et al., 1997; Beier et al., 2006). Rheological properties are modeled using a variable viscosity relationship for basaltic magma, parameterized in terms of temperature and water content (Giordano and Dingwell, 2003). MAGFLOW does not explicitly account for crystallization and lava composition, but these parameters are implicitly considered in the viscosity–temperature relationship.

Effusion rate curves defining the possible scenarios for the two eruptive classes ECL1 and ECL2 have been derived from the best fitting between actual and simulated lava flow fields of eruptions considered. The best fitting has been obtained using a bell-shaped effusion rate curve, reaching the peak after a 1/3 of the entire time of simulation and then gradually decreasing until the end of the eruption.

Finally, the nodes of the regular grid (whose area is displayed in Fig. 6a) have been considered as the locations of eruptive vents. From each potential vent, we have simulated both the case of ECL1 and of ECL2, characterized by different effusion rate curves.

4.4. Computation of the hazard by lava flow inundation

The hazard posed by lava flow inundation has resulted from the combination of the spatial probability of future vent opening, the occurrence probability associated with the classes of expected eruptions, and the overlapping of the simulated lava flow paths. At any pixel (x,y) of the DEM, the lava flow hazard has been computed by:

$$H_{xy} = \sum\nolimits_i \lambda(v_i)\Delta x \Delta y \cdot p_e(v_i) \cdot p_{xy}(v_i) \quad (2)$$

where $\lambda(v_i)$ is the spatial probability of activation of the potential vent v_i, Δx and Δy define the pixel size of the DEM, $p_e(v_i)$ is the event probability in v_i for the eruptive classes ECL1 and ECL2, and $p_{xy}(v_i)$ is 1 or 0 according to whether the pixel (x,y) is inundated or not by a lava flow originating from v_i (Favalli et al., 2009). We have simulated more than 1500 lava flow scenarios emitted from 794 different potential vents, and the resulting hazard map is shown in Fig. 6b.

The total hazard area is ~31 km^2, and the maximum distance simulated is ~7 km, from source vents located in the south–west corner of the grid, to Relva village (Fig. 6b). The highest hazard level (0.023) is reached between Santo António and Feteiras villages, following a NE–SW direction exactly perpendicular to the Éguas–Carvão volcanic system. Other areas more likely to be threatened by at least one lava flow are in the Covoada parish and in the Capelas village.

Due to the small number of past lava flows and the large uncertainty regarding their age, we have not considered absolute probabilities (i.e. probabilities within a specific time period), limiting our investigation

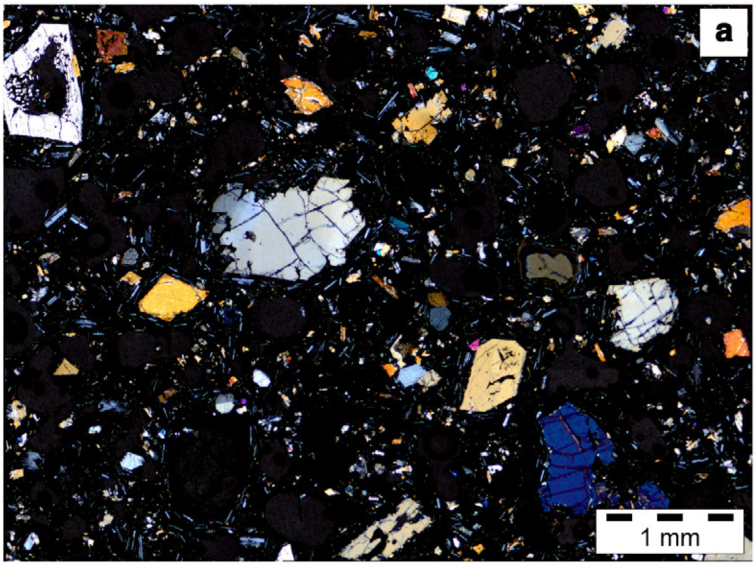

Sample	Mineral assemblage	Modal value
Picos das Éguas	**Xenocrysts and phenocrysts**	
	plg	*0.5*
	cpx	*11.6*
	ol	*12.0*
	ox	*1.2*
	Microphenocrysts	
	plg	*15.3*
	cpx	*9.4*
	ol	*2.3*
	ox	*8.4*
	Groundmass	*39.4*

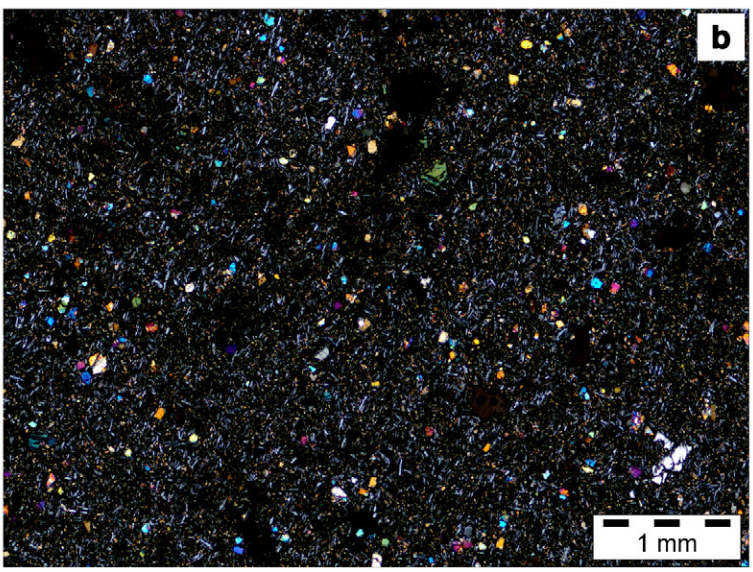

Sample	Mineral assemblage	Modal value
Pico do Carvão	**Phenocrysts**	
	cpx	*0.1*
	ol	*0.3*
	Microphenocrysts	
	plg	*14.3*
	cpx	*0.1*
	ol	*6.3*
	ox	*7.2*
	Groundmass	*71.6*

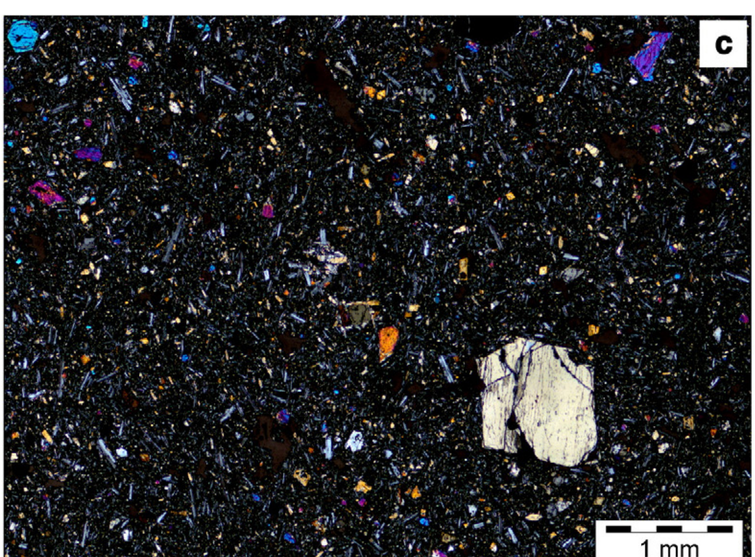

Sample	Mineral assemblage	Modal value
Picos das Ferrarias	**Xenocrysts**	
	plg	*1.0*
	cpx	*0.9*
	ol	*1.4*
	Phenocrysts	
	plg	*1.5*
	cpx	*1.4*
	ol	*2.4*
	Microphenocrysts	
	plg	*12.7*
	cpx	*3.1*
	ol	*6.3*
	ox	*5.5*
	Groundmass	*63.7*

to the assessment of constrained hazard. When past eruptions are accurately documented and well-dated, absolute probabilities could be obtained by introducing a multiplicative factor that depends on the recurrence rates, i.e. events expected × unit area × unit time (Del Negro et al., 2013).

5. Lava flow risk assessment

Risk assessment includes hazard assessment, followed by estimations of the vulnerability and values of the elements at risk (or exposure), all leading to the computation of risk as function of hazard, vulnerability and exposure. Therefore, the risk posed by lava flow inundation is defined as the combination of the probability of the occurrence of an effusive eruption and the harm that might follow (Fournier d'Albe, 1979). It can be mathematically expressed by the following dimensionless indexes:

$$R = H \times V \times E \tag{3}$$

where H is the hazard, V is the vulnerability, i.e. the evaluation of how much an element (e.g. people, buildings, infrastructure, economic activities) can be damaged by an eruptive event (Rapicetta and Zanon, 2008), and E is the exposure, i.e. the economic value of each element at risk. In general, the vulnerability varies from 0 to 1 depending on the hazardous phenomenon considered. In the case of a lava flow, it can be assumed to be 1, i.e. total loss of infrastructures upon impact by lava flows (Favalli et al., 2009, 2012).

The exposure index is a measure of the direct impact of lava flows on all elements in the area threatened by inundation. We have assessed the exposure by considering the population, the anthropogenic and the land use indexes. All indexes have been normalized, ranging from 0 to 1, and have been used to obtain the final exposure index with a weighted linear combination, assigning to each index the same weight (Alberico et al., 2011; Alcorn et al., 2013). Raw data have been collected from the Municipal Portal of Ponta Delgada (http://cm-pontadelgada.azoresdigital.pt).

The population index has been obtained by considering the number of inhabitants per square kilometer (from the 2001 census) living in each parish, possibly covered by future lava flows. The values obtained have been then rescaled as a function of the maximum value reached and homogeneously assigned within the municipal bounds (Fig. 7a).

The anthropogenic index indicates the presence of buildings and/or roads. It varies between 0 (complete absence) and 1 (maximum presence of buildings and roads). The number of buildings has been calculated by converting the vectorial geographical data to raster format, so that the value represented by each 30-m cell indicates how many buildings are at a limiting distance of 50 m from the center of the cell (Cappello, 2014). The value of each cell has been then normalized using the maximum value. The same approach has been used for roads. Finally, the distribution of anthropogenic factors on the territory has been obtained through a weighted sum, where the building and road rasters have a weight of 0.75 and 0.25, respectively (Fig. 7b).

The land use index classifies the area on the basis of the typology of soil occupation. Six categories have been identified according to their main use. In *agricultural areas* the main activity is harvesting and in *production areas* it is milking. The *natural space* category includes all zones that should be preserved due to the importance of the natural environment. Areas of economic or environmental interest are classified as *protected areas*. The zones around the protected areas are classified as *protection areas*. Constructions are not allowed in these last three areas. *Urban areas* are the sites where the main residential buildings are located, including future urbanization zones. We have assigned an increasing weight between zero and one to these six categories, with respect to the economic loss in case of lava flow inundation (Fig. 7c). The values of E for each area are shown in Fig. 7d.

Final values of risk, showing the likely damage upon the occurrence of a lava flow eruption, vary between 0 and 0.015. For many practical applications, however, it is more convenient and useful to consider a simplified map including a reduced number of risk classes (Cappello, 2014). To produce this simplified map, risk values are shown in logarithmic scale to highlight four main levels: high, medium, low and very low. The very low level was assigned to those areas not inundated by any simulated lava flow (Fig. 8).

6. Discussion and conclusions

The primary purpose of this work is to provide the first quantitative assessment of the hazard and risk posed by lava flow inundation from possible effusive eruptions in the island of São Miguel. We have showed how eruptive vents at the Éguas–Carvão fissure system may cause social and economic damage for the São Miguel Island.

The hazard map (Fig. 6b) shows the areas threatened by possible future lava flows from the Éguas–Carvão fissure system, covering more than 10 km^2 of built-up areas and 3500 km of roads, including degraded, dirt, and paved roads. Main urbanized areas exposed to lava inundation are Feteiras, Capelas and Santo Antonio. These are the main villages (with more than 7000 inhabitants) close to the Éguas–Carvão fissure system. On the other hand, the airport and the NW periphery of Ponta Delgada are not threatened by lava flows. Indeed, natural morphological barriers would channel the lava flows directly to the NE and SW slopes of this area of the RPFZ, saving the airport and Ponta Delgada surroundings from lava flows. The territory of the São Miguel Island is mainly classified as rural (http://www.azores.gov.pt/Portal/pt/entidades/srrn-dradr). Bovine farming is extensively practiced in the study area to ensure the sustenance of local population (meat and milk), with vast spaces reserved to grazing in the low slopes of the RPFZ, while agriculture consists of limited cereals crops and potatoes, mainly for private consumption. Hence, an effusive eruption would render this land sterile for long periods and force the moving of herds of cows to distant grazing areas.

The lava flow simulations show that villages located on the western side of the Sete Cidades volcano could be cut off from the rest of the island, forcing these communities to survive exclusively from their own resources. Furthermore, if the main road was cut a significant issue to the public health would be created, since the only hospital is in Ponta Delgada and no helicopter is available in the entire island. Food supply and first aid should rely on small fishing boats; however, many communities do not even have a small jetty for mooring boats. It is worth to note that the maps presented quantify the threat posed only by a subset of the possible future lava effusions. Hence, the exposed value considered (e.g. all the villages shown in Figs. 6–7) is clearly exposed also to possible lava flows originating from outside the area considered as source for future flows.

Obviously, the accuracy of our results strictly depends on the quality of field data, as input parameters in the MAGFLOW model (including the resolution of the DEM and the shape of the effusion rate curves), on the assumption of the same probability of occurrence to the eruptive classes, and on the limited extent of the area including the potential vents. Indeed, the investigated area is confined to the upper part of

Fig. 5. Petrographic characteristics of erupted products in the area of Éguas–Carvão fissure system are quite different in terms of crystal content and microstructure. The lavas from Pico das Éguas are highly porphyritic (a), with numerous mafic phases, both phenocrysts and xenocrysts. In the case of the products related to the eruption of the Pico do Carvão, the crystal content is reduced and there are no xenocrysts (b). The lavas emitted by the Picos das Ferrarias fissure system are crystal-poor and are similar to those emitted by Pico do Carvão, but contain more phenocrysts and scattered xenocrysts (c).

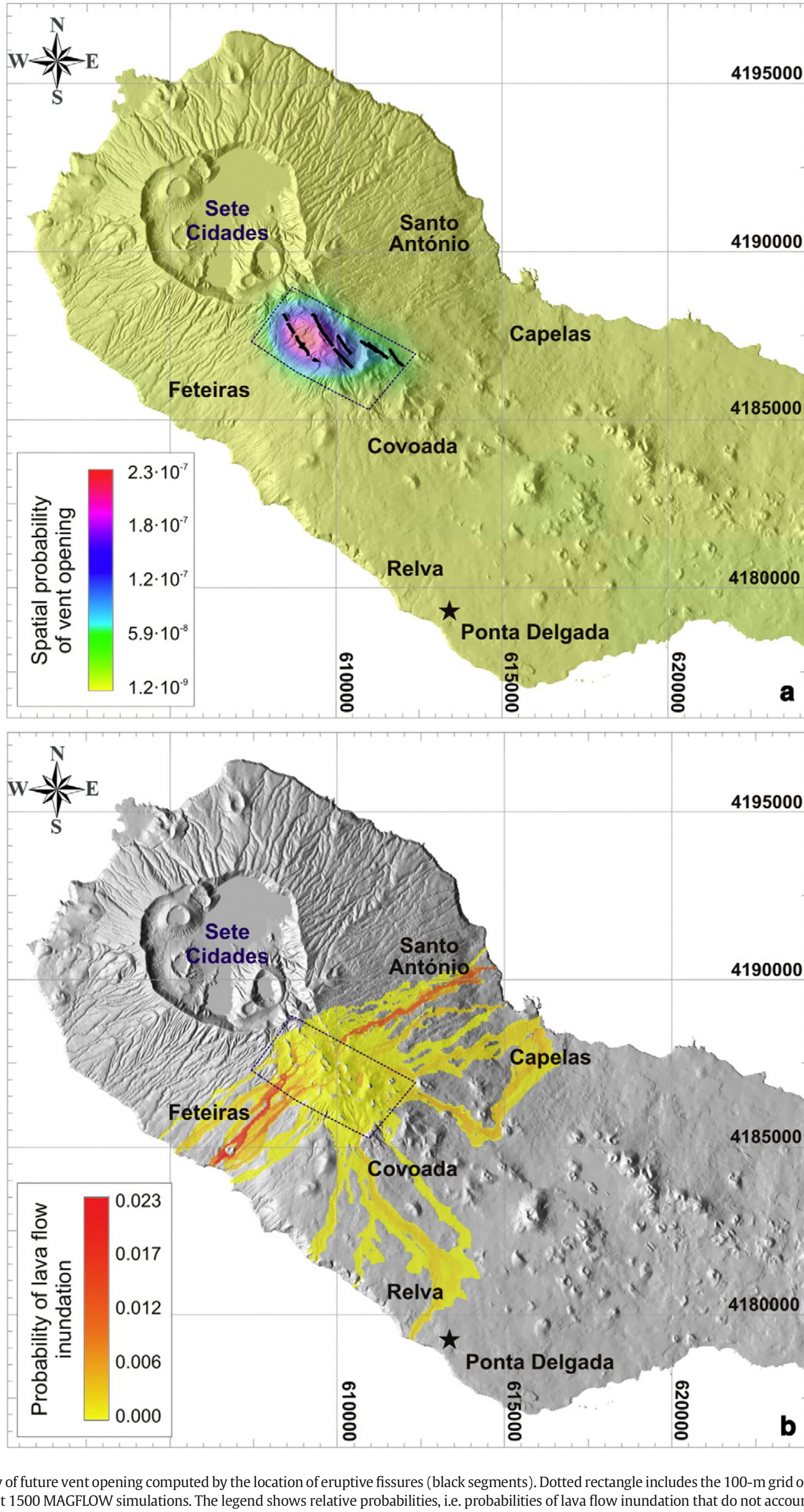

Fig. 6. a) Spatial probability of future vent opening computed by the location of eruptive fissures (black segments). Dotted rectangle includes the 100-m grid of potential vents; b) lava flow hazard map based on about 1500 MAGFLOW simulations. The legend shows relative probabilities, i.e. probabilities of lava flow inundation that do not account for the temporal likelihood of eruptions. The black star marks the location of Ponta Delgada airport.

Table 2
Input parameters for the MAGFLOW simulations of lava flow paths.

Parameter	Value	Unit of measurement
Density of lava	2900 for ECL1–2500 for ECL2	kg m^{-3}
Specific heat capacity	1150	J kg^{-1} K^{-1}
Emissivity	0.9	–
Solidification temperature	1100	K
Extrusion temperature	1475	K

System I, i.e. the rift zone closest to the Sete Cidades caldera. This choice is motivated by the more recent historical volcanic activity occurred at the Éguas–Carvão fissure system, as well as a much higher spatial frequency of eruptive fissures. Clearly, an eruptive vent may also open on the distal portion of System I, near Ponta Delgada, increasing the risk from lava flow inundation. Nevertheless, the products of our analysis, lava flow hazard and risk maps can be useful tools to provide operational guidelines for mitigation during eruptive emergencies. Moreover, these maps may also encourage a better planning of land use. Clearly a hazard map does not provide a deterministic forecast of future eruptions, but it rather makes a useful prediction based on modeling of historical eruptive activity of a volcano. Such maps are thus an essential guide in managing volcanic emergencies in terms of planning, mitigation of potential effects, relief efforts and assessing potential loss and restoration costs.

Acknowledgments

This work was developed in the frame of the TechnoLab, the Laboratory for the Technological Advance in Volcano Geophysics organized by INGV-CT and UNICT (Italy). It was partially funded by the Fundação para a Ciência e Tecnologia—Portugal (Project no. PTDC/CTE-GIX/098836/2008). The orthophotos used in this work were kindly provided by the Regional Government of the Azores, through an agreement with the CVARG. V. Zanon was funded by FRCT through grant 03.1.7.2007.1 (FRCT-PROEMPREGO Operational Program and Regional Government of the Azores). Ana Gomez and Massimiliano Porreca provided a valid help during field work and Ana Rita Mendes during samples preparation for petrographic analysis. ASTER GDEM is a product of METI and NASA. The Associate Editor Joan Martí, two anonymous reviewers and Gabor

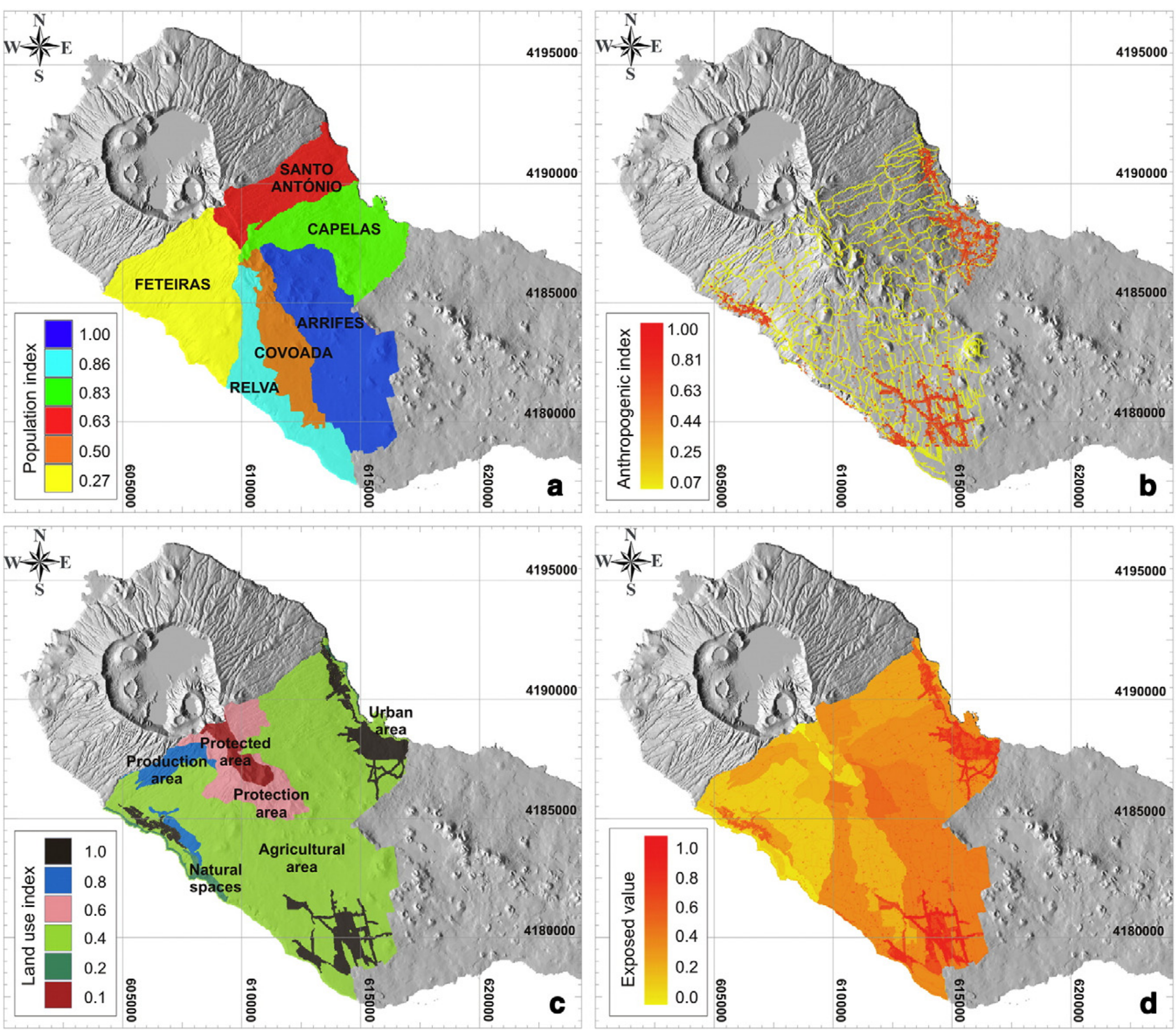

Fig. 7. a) Population index obtained as a percentage density of inhabitants per parish; b) raster map showing the distribution of anthropogenic factors (buildings and roads); c) land use index obtained by categorizing the territory on the basis of ground coverage; d) exposed value calculated as the normalized sum of the population, anthropogenic and land use indices.

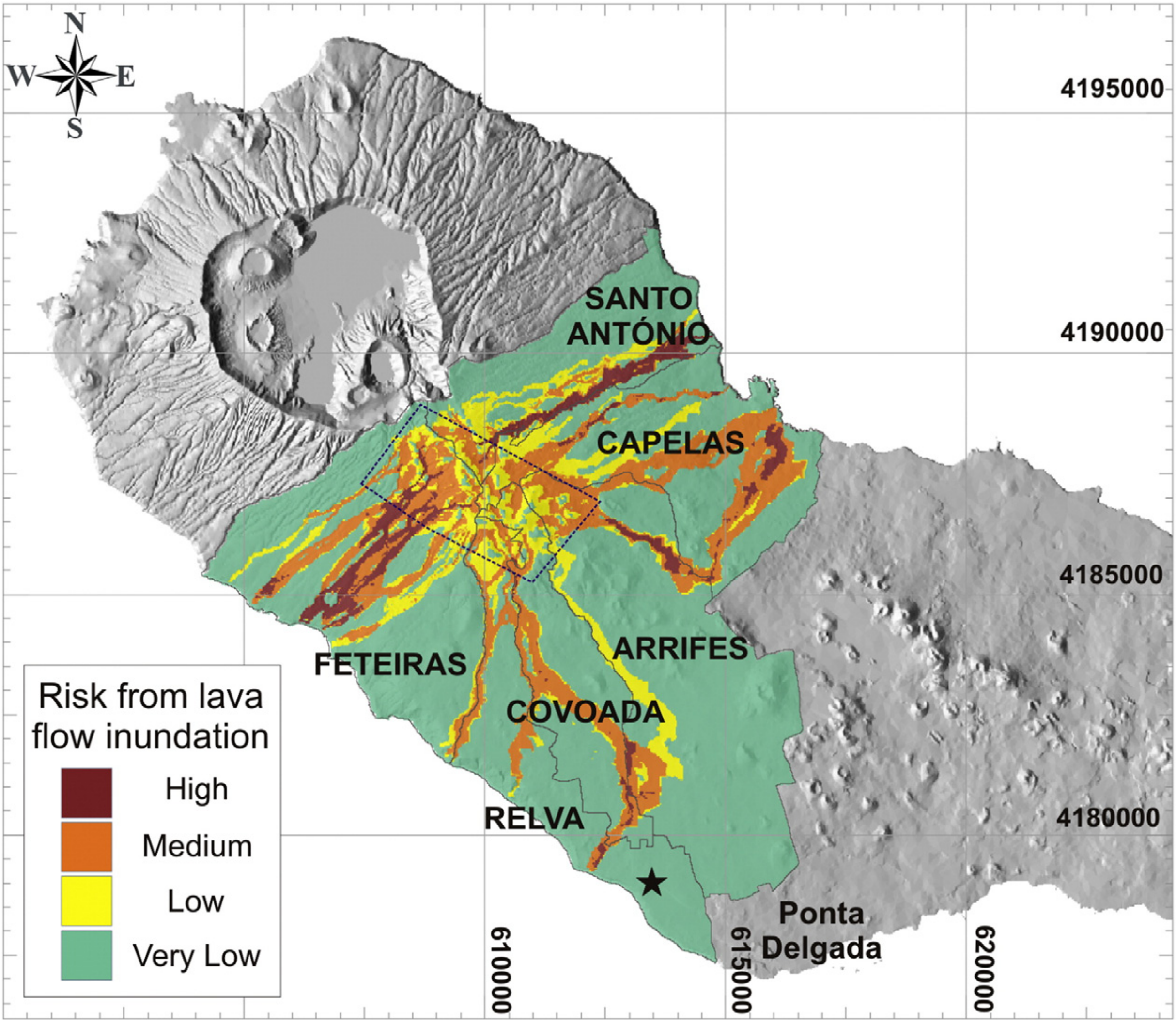

Fig. 8. Lava flow risk map obtained by multiplying the hazard map with the exposed value. The logarithmic scale is applied to improve the map readability. Gray lines delimit the boundaries of parishes. Dotted rectangle includes the locations of potential vents and the black star marks the Ponta Delgada airport.

Kereszturi are acknowledged for their constructive and supportive comments that helped us significantly improve the manuscript.

References

Alberico, I., Petrosino, P., Lirer, L., 2011. Volcanic hazard and risk assessment in a multi-source volcanic area: the example of Napoli city (southern Italy). Nat. Hazards Earth Syst. Sci. 11, 1057–1070.

Alcorn, R., Panter, K.S., Gorsevski, P.V., 2013. A GIS-based volcanic hazard and risk assessment of eruptions sourced within Valles Caldera, New Mexico. J. Volcanol. Geotherm. Res. 267, 1–14.

Bartolini, S., Cappello, A., Martí, J., Del Negro, C., 2013. QVAST: a new Quantum GIS plugin for estimating volcanic susceptibility. Nat. Hazards Earth Syst. Sci. 13, 3031–3042. http://dx.doi.org/10.5194/nhess-13-3031-2013.

Becerril, L., Cappello, A., Galindo, I., Neri, M., Del Negro, C., 2013. Spatial probability distribution of future volcanic eruptions at El Hierro Island (Canary Islands, Spain). J. Volcanol. Geotherm. Res. 257, 21–30.

Beier, C., Haase, K.M., Hansteen, T.H., 2006. Magma evolution of the Sete Cidades volcano, São Miguel, Azores. J. Petrol. 47, 1375–1411.

Bilotta, G., Cappello, A., Hérault, A., Vicari, A., Russo, G., Del Negro, C., 2012. Sensitivity analysis of the MAGFLOW Cellular Automaton model for lava flow simulation. Environ. Model Softw. 35, 122–131.

Cappello, A., 2014. Probabilistic Modelling of Lava Flow Hazard at Mount Etna. Scholars' Press 978-3-639-66289-4, p. 188.

Cappello, A., Vicari, A., Del Negro, C., 2011a. Assessment and modeling of lava flow hazard on Etna volcano. Boll. Geofis. Teor. Appl. 52 (2), 299–308. http://dx.doi.org/10.4430/bgta0003.

Cappello, A., Vicari, A., Del Negro, C., 2011b. Retrospective validation of a lava flow hazard map for Mount Etna volcano. Ann. Geophys. 54 (5). http://dx.doi.org/10.4401/ag-5345.

Cappello, A., Neri, M., Acocella, V., Gallo, G., Vicari, A., Del Negro, C., 2012. Spatial vent opening probability map of Etna volcano (Sicily, Italy). Bull. Volcanol. 74 (9), 2083–2094.

Cappello, A., Bilotta, G., Neri, M., Del Negro, C., 2013. Probabilistic modelling of future volcanic eruptions at Mount Etna. J. Geophys. Res. Solid Earth 118, 1–11. http://dx.doi.org/10.1002/jgrb.50190.

Cole, P.D., Guest, J.E., Queiroz, G., Wallenstein, N., Pacheco, J.M., Gaspar, J.L., Ferreira, T., Duncan, A.M., 1999. Styles of volcanism and volcanic hazards on Furnas volcano, São Miguel, Azores. J. Volcanol. Geotherm. Res. 92 (1–2), 39–53.

Cole, P.D., Pacheco, J.M., Gunasekera, R., Queiroz, G., Gonçalves, P., Gaspar, J.L., 2008. Contrasting styles of explosive eruption at Sete Cidades, São Miguel, Azores, in the last 5000 years: hazard implications from modelling. J. Volcanol. Geotherm. Res. 178, 574–591.

Crisci, G.M., Avolio, M.V., Behncke, B., D'Ambrosio, D., Di Gregorio, S., Lupiano, V., Neri, M., Rongo, R., Spataro, W., 2010. Predicting the impact of lava flows at Mount Etna, Italy. J. Geophys. Res. 115, B04203. http://dx.doi.org/10.1029/2009JB006431.

Del Negro, C., Fortuna, L., Herault, A., Vicari, A., 2008. Simulations of the 2004 lava flow at Etna volcano using the magflow cellular automata model. Bull. Volcanol. 70 (7), 805–812.

Del Negro, C., Cappello, A., Neri, M., Bilotta, G., Herault, A., Ganci, G., 2013. Lava flow hazards at Mount Etna: constraints imposed by eruptive history and numerical simulations. Sci. Rep. 3, 3089. http://dx.doi.org/10.1038/srep03493.

Favalli, M., Mazzarini, F., Pareschi, M.T., Boschi, E., 2009. Topographic control on lava flow paths at Mount Etna, Italy: implications for hazard assessment. J. Geophys. Res. 114, F01019.

Favalli, M., Tarquini, S., Papale, P., Fornaciai, A., Boschi, E., 2012. Lava flow hazard and risk at Mt. Cameroon volcano. Bull. Volcanol. 74 (2), 423–439.

Felpeto, A., Araña, V., Ortiz, R., Astiz, M., García, A., 2001. Assessment and modelling of lava flow hazard on Lanzarote (Canary Islands). Nat. Hazards 23 (2–3), 247.

Ferreira, T., 2000. Caracterização da actividade vulcânica da ilha de São Miguel (Açores): vulcanismo basáltico recente e zonas de desgaseificação. Avaliação de riscos. Departemento de Geociências. University of Azores, Ponta Delgada, p. 248.

Fournier d'Albe, E.M., 1979. Objectives of volcanic monitoring and prediction. J. Geol. Soc. 136 (3), 321–326.

Ganci, G., Vicari, A., Cappello, A., Del Negro, C., 2012. An emergent strategy for volcano hazard assessment: from thermal satellite monitoring to lava flow modeling. Remote Sens. Environ. 119, 197–207. http://dx.doi.org/10.1016/j.rse.2011.12.021.

Gehl, P., Quinet, C., Le Cozannet, G., Kouokam, E., Thierry, P., 2013. Potential and limitations of risk scenario tools in volcanic areas through an example at Mount Cameroon. Nat. Hazards Earth Syst. Sci. 13, 2409–2424.

Giordano, D., Dingwell, D., 2003. Viscosity of hydrous Etna basalt: implications for Plinian-style basaltic eruptions. Bull. Volcanol. 65 (1), 8–14.

Guest, J.E., Gaspar, J.L., Cole, P.D., Queiroz, G., Duncan, A.M., Wallenstein, N., Ferreira, T., Pacheco, J.M., 1999. Volcanic geology of Furnas Volcano, São Miguel, Azores. J. Volcanol. Geotherm. Res. 92 (1–2), 1–29.

Herault, A., Vicari, A., Ciraudo, A., Del Negro, C., 2009. Forecasting lava flow hazards during the 2006 Etna eruption: using the MAGFLOW cellular automata model. Comput. Geosci. 35 (5), 1050–1060.

Johnson, C.L., Wijbrans, J.R., Constable, C.G., Gee, J., Staudigel, H., Tauxec, L., Forjaz, V.H., Salgueiro, M., 1998. $^{40}Ar/^{39}Ar$ ages and paleomagnetism of São Miguel lavas, Azores. Earth Planet. Sci. Lett. 160 (3–4), 637–649.

Kauahikaua, J., Margriter, S., Lockwood, J., Trusdell, F., 1995. Applications of GIS to the estimation of lava flow hazard on Mauna Loa Volcano, Hawaii. In: Rhodes, J.M., Lockwood, J.P. (Eds.), Mauna Loa revealed: structure, composition, history, and hazards. American Geophysical Union Geophysical Monograph 92, pp. 315–325.

Kereszturi, G., Cappello, A., Ganci, G., Procter, J., Németh, K., Del Negro, C., Cronin, S.J., 2014. Numerical simulation of basaltic lava flows in the Auckland Volcanic Field, New Zealand—implication for volcanic hazard assessment. Bull. Volcanol. 76, 879. http://dx.doi.org/10.1007/s00445-014-0879-6.

Kilburn, C.R.J., 2000. Lava flows and flow fields. In: Sigurdsson, H., Houghton, B.F., McNutt, S.R., Rymer, H., Stix, J. (Eds.), Encyclopedia of Volcanoes. Academic Press, pp. 291–306.

Lourenço, N., Miranda, J.M., Luis, J.F., Ribeiro, A., Mendes Victor, L.A., Madeira, J., Needham, H.D., 1998. Morpho-tectonic analysis of the Azores Volcanic Plateau from a new bathymetric compilation of the area. Mar. Geophys. Res. 20, 141–156.

Luis, J.F., Miranda, J.M., Galdeano, A., Patriat, P., 1998. Constraints on the structure of the Azores spreading center from gravity data. Mar. Geophys. Res. 20, 157–170.

Madeira, J., Brum da Silveira, A., 2003. Active tectonics and first paleoseismological results in Faial, Pico and S. Jorge Islands (Azores, Portugal). Ann. Geophys. 46 (5), 733–761.

Madeira, J., Ribeiro, A., 1990. Geodynamic models for the Azores triple junction. A contribution from tectonics. Tectonophysics 184 (3–4), 405–415.

Marques, F.O., Catalão, J.C., DeMets, C., Costa, A.C.G., Hildenbrand, A., 2013. GPS and tectonic evidence for a diffuse plate boundary at the Azores Triple Junction. Earth Planet. Sci. Lett. 381, 177–187.

Mattioli, M., Upton, B.G.J., Renzulli, A., 1997. Sub-volcanic crystallization at Sete Cidades volcano, Miguel, Azores, inferred from mafic and ultramafic plutonic nodules. Mineral. Petrol. 60, 1–26.

Miranda, J.M., Mendes Victor, L.A., Simões, J.Z., Luis, J.F., Matias, L., Shimamura, H., Shiobara, H., Nemoto, H., Mochizuki, H., Hirn, A., Lépine, J.C., 1998. Tectonic setting of the Azores plateau deduced from a OBS survey. Mar. Geophys. Res. 20, 171–182.

Moore, R.B., 1990. Volcanic geology and eruption frequency, São Miguel, Azores. Bull. Volcanol. 52, 602–614.

Moore, R.B., Rubin, A.M., 1991. Radiocarbon dates for lava flows and pyroclastic deposits on São Miguel, Azores. Radiocarbon 33 (1), 151–164.

Queiroz, G., Pacheco, J.M., Gaspar, J.L., Aspinall, W.P., Guest, J.E., Ferreira, T., 2008. The last 5000 years of activity at Sete Cidades volcano (S. Miguel Island, Azores): implications for hazard assessment. J. Volcanol. Geotherm. Res. 178, 562–573.

Rapicetta, S., Zanon, V., 2008. GIS-based method for the environmental vulnerability assessment to volcanic ashfall at Etna Volcano. Geoinformatica 13, 267–276.

Vicari, A., Herault, A., Del Negro, C., Coltelli, M., Marsella, M., Proietti, C., 2007. Modeling of the 2001 lava flow at Etna volcano by a Cellular Automata approach. Environ. Model Softw. 22 (10), 1465–1471.

Vicari, A., Ciraudo, A., Del Negro, C., Herault, A., Fortuna, L., 2009. Lava flow simulations using discharge rates from thermal infrared satellite imagery during the 2006 Etna eruption. Nat. Hazards 50 (3), 539–550.

Vicari, A., Ganci, G., Behncke, B., Cappello, A., Neri, M., Del Negro, C., 2011. Near-real-time forecasting of lava flow hazards during the 12–13 January 2011 Etna eruption. Geophys. Res. Lett. 38 (13), L13317.

Worton, B.J., 1995. Using Monte Carlo simulation to evaluate kernel-based home range estimators. J. Wildl. Manag. 59, 794–800.

Zanon, V., 2014. Conditions for mafic magma storage beneath fissure zones at oceanic islands. The case of São Miguel island (Azores archipelago). J. Geol. Soc. Lond. (in press).